Check for updates

ADVANCED SUSTAINABLE SYSTEMS
www.advsustainsys.com

Nature-Inspired Depolymerization of Soda Lignin: Light-Induced Free Radical Promoted Cleavage of β-O-4 Bonds

Kerem Kaya, Armagan Atsay, Hande Gunduz, Adam Slabon, and Yusuf Yagci*

This paper is dedicated to the memory of Professor Yusuf Yagci

The development of sustainable valorization methods for lignin is a challenging task because the vast majority of the reported studies involve either harsh conditions or expensive transition metal catalysts. Inspired by the sunlight degradation of lignin compounds, known as lignin yellowing, the use of a commercially available cheap organic photoinitiator, namely, phenacyl bromide (PAB) is reported here, for the efficient cleavage of lignin model compound 2-phenoxyacetophenone (2-PAP) and for the depolymerization of soda pulped lignin (SL) under UV-A irradiation and ambient conditions. Real-time NMR investigations of the photoreaction between 2-PAP and PAB shed light on the possible reaction mechanisms involving different radical species, HBr, and molecular oxygen. Interestingly, combined spectral, chromatographic, powder X-ray diffraction, and thermal studies of the photoreaction between PAB and SL indicate the formation of guaiacyl alcohol as the main product. The unprecedented performance of PAB is attributed to the excess generation of phenacyl radicals, the generation of photolabile brominated species, and HBr playing key roles in the cleavage of β-O-4 linkages. This work represents a new edge for sustainable lignin valorization under mild reaction conditions and offers the opportunity for large-scale production of valuable aromatics using technical lignins as feedstock.

1. Introduction

The excessive use of fossil resources contributes to environmental pollution which is suspected to be the main reason for global warming.[1] Therefore, it is highly relevant to find alternative renewable energy sources to mitigate global warming, which can commit over one-third of the Earth's animal and plant species to extinction within 25 years.[2]

Lignocellulosic biomass has received significant interest in recent years due to its potential application as second-generation biofuels and CO_2-neutral renewable feedstock for platform chemicals and materials.[3] Lignin, being one of the three main constituents of the plant cell walls, is the largest biomass of aromatic compounds.[4] However, it is a great challenge to produce monomers from lignin compounds due to their extremely complex, three-dimensional, and cross-linked structure formed mainly by the radical coupling reactions of monolignols which are p-hydroxyphenyl (H), guaiacyl (G), and syringyl (S) units.[5] In fact, there are hundreds of research articles dedicated to the structural characterization of different lignin compounds using various chromatographic or spectroscopic techniques.[6]

Technical lignins are by-products of paper and pulp industry. They are obtained by different pulping techniques such as soda, kraft, and organosolv.[7] Soda lignin (SL) has the main advantage of being sulfur-free, thus, having a similar structure to that of native lignin.[8] Owing to its high purity and biocompatibility, SL has been used in different applications, including the production

K. Kaya, A. Atsay, Y. Yagci
Chemistry Department
Istanbul Technical University
Istanbul 34469, Turkey
E-mail: kkaya@itu.edu.tr

The ORCID identification number(s) for the author(s) of this article can be found under https://doi.org/10.1002/adsu.202300366

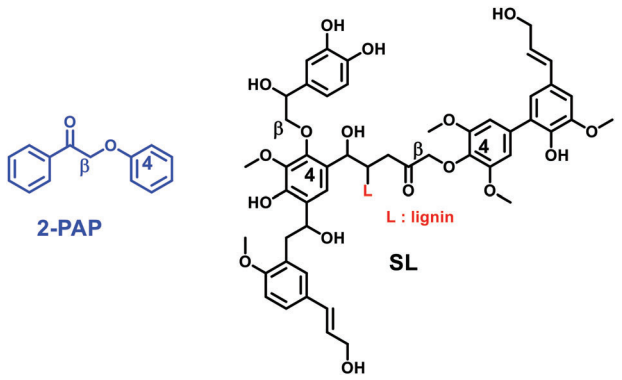
© 2023 The Authors. Advanced Sustainable Systems published by Wiley-VCH GmbH. This is an open access article under the terms of the Creative Commons Attribution-NonCommercial License, which permits use, distribution and reproduction in any medium, provided the original work is properly cited and is not used for commercial purposes.

DOI: 10.1002/adsu.202300366

K. Kaya
Department of Materials and Environmental Chemistry (MMK)
Stockholm University
Stockholm 10691, Sweden

H. Gunduz
Chemistry Department
Koc University
Istanbul 34450, Turkey

A. Slabon
Inorganic Chemistry
University of Wuppertal
42119 Wuppertal, Germany



Scheme 1. Structures of 2-PAP and soda lignin (SL) with β-O-4 linkages.

of dispersants, phenolic resins, and animal food. Nonetheless, around 99% of all the technical lignins that could actually become the source of many other value-added aromatic compounds, are currently used as cheap fuel for burning.

β-O-4 (C—O—C) ether bonds are the most abundant linkages in lignin (≈60%).[5a,9] Consequently, cleavage of these etheric bonds can significantly enhance the yield of valuable aromatic monomers.[10] Especially in the last two decades, many efforts have been devoted to the valorization of lignin by taking advantage of β-O-4 bond cleavage reactions.[11] Nevertheless, due to the complexity of lignin's structure, scientists have mostly investigated the cleavage reactions on lignin model compounds containing β-O-4 bonds, such as 2-phenoxyacetophenone (2-PAP).[12] Structures of 2-PAP and SL can be seen in **Scheme 1**, even though SL's real structure is much more complicated.

Most of the current methods of lignin/model compounds valorization/cleavage involve chemical oxidation/reduction reactions performed under harsh conditions using expensive/toxic chemicals and/or elevated temperatures.[13] Electrochemical reactions, despite their efficiency, suffer mostly from the necessity of sophisticated equipment which limits their large-scale applications.[14] Given all these challenges, it is obvious that sustainable lignin valorization still remains a difficult task if one aims to substitute current platform chemicals in the industry.

In the context of Sustainable Chemistry,[15] light-induced valorization of lignin has recently garnered significant interest due to the milder reaction conditions and higher efficiency.[16] This has been lately achieved by several groups using different semiconductors on model compounds mostly under an inert atmosphere. However, only a few studies have reported the valorization of lignin compounds using metal-free and ambient conditions.[17]

It has been previously demonstrated that phenacyl and ketyl radicals formed by sunlight exposure in UV-A region (>300 nm) can initiate the degradation of wood materials like lignin through β-O-4 cleavage, resulting in the phenomenon called lignin yellowing.[18] Moreover, electron spin resonance (ESR) investigations have revealed the sensitivity of lignin model compounds to Norrish type I cleavage and the crucial role of phenacyl/ketyl radicals in these cleavage reactions, especially under air atmosphere rather than nitrogen atmosphere.[19] Yet, lignin's dark color blocks UV light due to the presence of highly absorbing chromophore groups such as conjugated phenolics, ketones, and quinoids.[20] Indeed, structurally modified lignin has been used as a UV-protective material in sunscreens.[21] Low penetration of UV light into lignin causes a severe limitation to the formation of further phenacyl/ketyl radicals rendering the natural degradation of lignin insufficient for the valorization.

Alternatively, halogenated compounds are known to be photolabile due to their broader light absorption wavelengths and higher absorption coefficients.[22] Therefore, in order to accelerate and enhance light-induced cleavage reactions, brominated species, capable of promoting free radical reactions,[23] are usually incorporated into polymer chains.[24] In addition, bromination of lignin moieties can remarkably reduce their aggregation through $\pi-\pi$ stacking, by causing steric hindrance and resulting in improved solubility.[25] Lastly, brominated aromatic species are known to trigger the formation of reactive oxygen species (ROS), potent molecules that are known to play a crucial role in cleavage reactions.[26]

In light of the above considerations, we envisioned that simultaneous generation of phenacyl radicals and bromination could provide efficient photocleavage reactions. In this work, we report the use of a simple and commercially available cheap organic photoinitiator, namely phenacyl bromide (PAB), for the light-induced cleavage of 2-PAP and successive depolymerization of SL under UV-A irradiation yielding mainly guaiacyl alcohol at ambient conditions. Contrary to most of the previously reported light-induced valorization methods of lignin, this work does not involve any expensive/toxic transition metal catalyst or inert atmosphere. Real-time nuclear magnetic resonance (NMR) investigations of model compound (2-PAP) cleavage along with other spectroscopic and chromatographic data shed light on the possible photoreaction mechanism for the SL depolymerization.

2. Results and Discussion

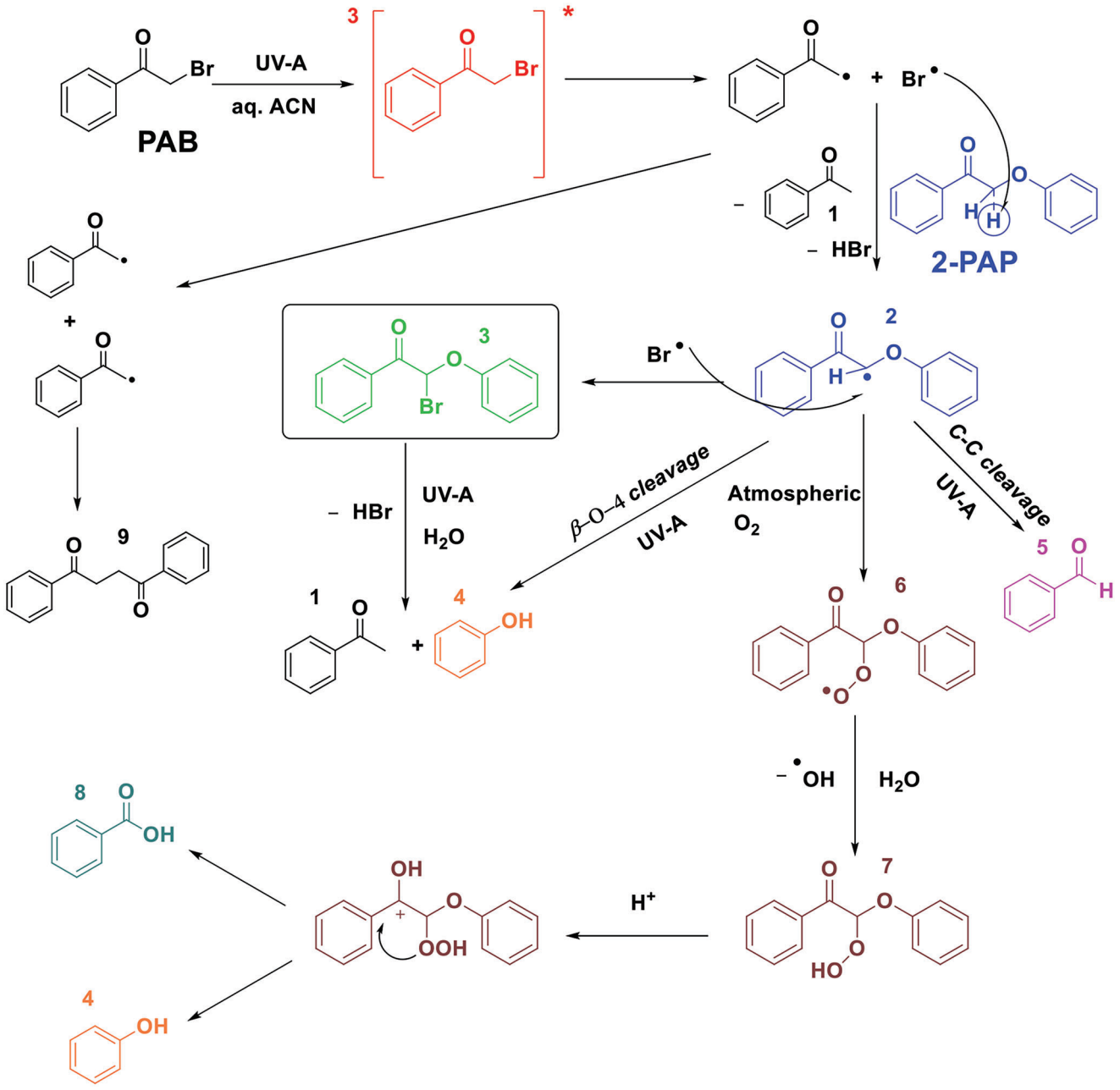
PAB is a multi-purpose photoactive compound,[27] recently used for the photoinduced step-growth polymerization of a variety of aromatic monomers through the abstraction of electrons by photolytically generated bromine radical.[28] However, to our knowledge, the efficiency of PAB in cleavage/depolymerization reactions has not been previously investigated. Light-mediated cleavage of β-O-4 linkages, using PAB, was first investigated on lignin model compound 2-PAP, due to its purity and its much simpler structure compared to that of SL. At ambient conditions (room temperature and air atmosphere), reacting 2-PAP in the presence of 1.1 equiv. of PAB in aqueous acetonitrile (ACN) solvent led to a color change from yellow to dark orange after 4 h of UV-A irradiation (≈355 nm) inside a photoreactor (Figures S1 and S2, Supporting Information). The choice of aqueous ACN is due to its relatively safe nature, SL's moderate solubility in this solvent, and water being an important component of paper matrix.

^{1}H NMR spectra taken in $CDCl_3$, reveal the disappearance of —CH_2 peak of 2-PAP (5.28 ppm) and appearance of —CH_3 peak of acetophenone (2.6 ppm) after 4 h. (Figure S3, Supporting Information). In order to gain insight into the reaction mechanism, real-time ^{1}H NMR of the photocatalytic reaction between 2-PAP and PAB inside an NMR tube was employed using deuterated ACN (Figure S4, Supporting Information). Taking into consideration NMR and LC-HRMS (Liquid-chromatography high-resolution mass spectroscopy) (Figure S5, Supporting Informa-

© 2023 The Authors. Advanced Sustainable Systems published by Wiley-VCH GmbH

23667486, 0, Downloaded from https://onlinelibrary.wiley.com/doi/10.1002/adsu.202300366 by Koc University, Wiley Online Library on [23/03/2024]. See the Terms and Conditions (https://onlinelibrary.wiley.com/terms-and-conditions) on Wiley Online Library for rules of use; OA articles are governed by the applicable Creative Commons License

23667486, 0, Downloaded from https://onlinelibrary.wiley.com/doi/10.1002/adsu.202300366 by Koc University, Wiley Online Library on [23/03/2024]. See the Terms and Conditions (https://onlinelibrary.wiley.com/terms-and-conditions) on Wiley Online Library for rules of use; OA articles are governed by the applicable Creative Commons License



Scheme 2. Proposed reaction pathways for the photocleavage of 2-PAP.

tion) data obtained, we propose the following reaction mechanisms which are depicted in **Scheme 2**.

Accordingly, UV-A irradiation of PAB leads to the generation of bromine and phenacyl radicals through PAB's excited triplet state in high quantum yields, as previously demonstrated by Scaiano[29] and our group.[28a] Subsequent abstraction of methylene hydrogen of 2-PAP by readily formed bromine radical and the abstraction of proton by phenacyl radical from possibly aqueous solvent led to the production of radical compound (2) HBr, and acetophenone (1), respectively. Then, compound 2 couples with the bromine radical resulting in the chiral brominated product (3) which was confirmed by both 2D-HSQC NMR spectrum (Figure S6, Supporting Information) and LC-HRMS (Figure S5, Supporting Information). It was previously demonstrated, as discussed in the introduction part, that carbonyl-containing brominated aromatic compounds can homolytically cleave under UV irradiation provoking a scission reaction. In this case, the slow disappearance of compound 3 was observed in ^{1}H NMR spectrum (Figure S4, Supporting Information), leading to acetophenone (1) and phenol (4) through β-O-4 cleavage of compound 2. Benzaldehyde (5) which should be the product of C-C bond cleavage of compounds 2 and 3, was also identified both in ^{1}H NMR (Figure S3, Supporting Information peaks at 10 ppm, 8.0 ppm, 7.5 ppm) and LC-HRMS (Figure S5, Supporting Information). A

© 2023 The Authors. Advanced Sustainable Systems published by Wiley-VCH GmbH

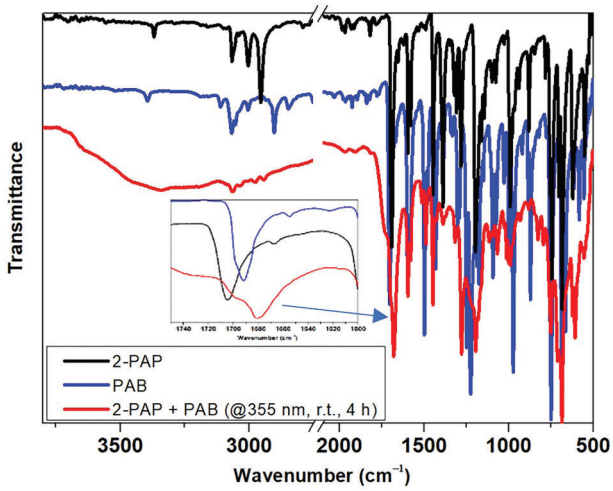


Figure 1. FT-IR spectra of (blue) 2-PAP, (black) PAB, and (red) 2-PAP + PAB @ 355 nm irradiation (inset image is focused on 1600–1800 cm^{-1}).

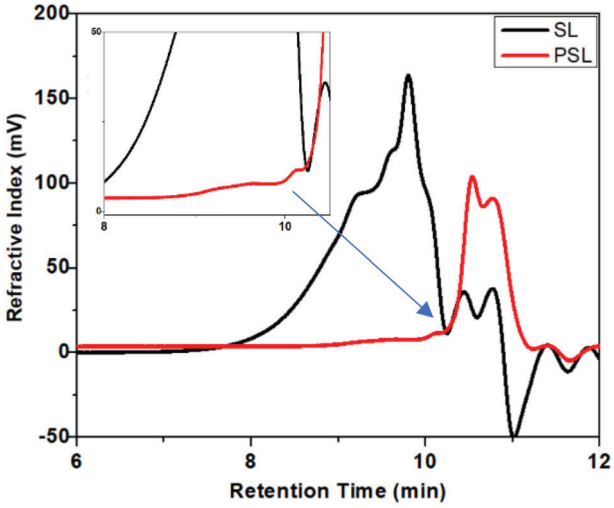


Figure 2. Lignin depolymerization analysis: GPC traces (in THF) obtained for (black) SL and (red) PSL using a refractive index detector (inset image is zoomed on GPC traces detected at 8–10 min intervals).

possible route for benzoic acid (8) observed in LC-HRMS might be the following; Compound 1 reacts with atmospheric oxygen to form the peroxy radical (6) which subsequently abstracts hydrogen from water molecules present in the solvent to generate compound 7 which is attacked by H^+ (coming from HBr), and transformed to benzoic acid (8) and phenol (4). Initial pH = 4.9 dropped to a final pH = 3.4 at the end of the photocatalytic reaction confirming the HBr release. The darkening of the reaction mixture's color can be attributed to the trace formation of coupling species (compound 9 and compound with m/z = 370) and to the formation of brominated compounds (3) having higher absorption coefficients (Figure S7, Supporting Information). The control experiment performed in the absence of PAB under identical reaction conditions did not show any significant change in ^{1}H NMR spectrum underlining the important role of PAB in the cleavage reactions (Figure S8, Supporting Information).

In the comparison of IR spectra of 2-PAP and its photoproducts (**Figure 1**), there is a clear broadening in the 3600–3400 cm^{-1} region corresponding to —OH group of phenol. The second most obvious difference in IR spectrum can be observed in the carbonyl region (1600–1750 cm^{-1}) due to the formation of acetophenone (1), benzaldehyde (5), and benzoic acid (8) having C═O stretching peaks at 1682 cm^{-1}, 1700 cm^{-1} and 1735 cm^{-1}, respectively (Figure 1 inset).

In a nutshell, photoreaction of 2-PAP with PAB consumed most of the 2-PAP, yielding acetophenone as the major product (from the photocleavage of both 2-PAP and PAB) along with phenol, benzaldehyde, benzoic acid, coupling species as side products. Encouraged by these results, we next attempted to cleave SL using PAB under similar conditions. As previously described in Scheme 2, two major routes are expected; a redox neutral process that cleaves β-O-4 bonds in Norrish type I manner and an oxidation process that produces different carbonyl compounds through the interaction of radical species with molecular oxygen (O_2). In a typical experiment, 64 mg of SL (2×10^{-5} mol according to GPC result) was mixed with 20 mg of PAB (1×10^{-4} mol) in 5 mL of aqueous ACN inside a 25 mL round-bottom flask with an open neck, and the solution was irradiated for 8 h under continuous stirring, inside the same photoreactor used for the 2-PAP, under ambient conditions. After the photoreaction, ACN solvent was evaporated from the dark brown colored mixture resulting in an oily (highly viscous) liquid (Figure S9, Supporting Information).

Different spectral, chromatographic, diffractometric, and thermal investigations were employed in order to speculate on the photoproducts of SL (PSL). First, a gel-permeation chromatography (GPC) investigation was performed to compare the chromatograms of SL and PSL (**Figure 2**). While GPC traces of SL contained high molecular weight fractions (M_n ≈3.24 kDa) with high dispersity ($Đ$ = 1.78), GPC traces of PSL mainly exhibited a M_n shift from ≈3.24 kDa to ≈0.13 kDa and a dispersity of $Đ$ = 1.08. Furthermore, area corresponding to low molecular weight fractions increased significantly in the chromatogram of PSL compared to those of SL indicating the formation of monomeric species and, thus, successful depolymerization.

Following GPC investigation, direct injection LC-HRMS analysis was employed to get insight into the possible depolymerization products (**Figure 3**a,b). Direct injection doesn't require any sample pre-treatment and the required sample volume is much smaller (100 µL) than a sample requiring pre-treatment (10 mL), thus improving the depth and time resolution that can be attained from lignin compounds.[30] It is possible to observe, looking at Figure 3a, that SL is not a random polymer since there is constant regularity along the whole mass spectrum (m/z = 217 to 833) with a difference of 44.03 m/z, which corresponds to C_2H_4O units.[31] This finding evidences that the soluble part of SL is formed by oligomeric species. On the other hand, mass spectrum of PSL shows a strong peak at m/z = 187.10 corresponding to lithium adduct of guaiacyl alcohol, according to literature,[32] and other peaks at higher m/z with much lower intensity.[33] Adducts such as lithium, sodium, and potassium are usually encountered in electrospray ionization (ESI) due to mobile phase, solvent impurities, or glassware.[34] Higher m/z values are not related to the peaks observed in SL's mass spectrum indicating structural changes in SL and the possible presence of brominated species

© 2023 The Authors. Advanced Sustainable Systems published by Wiley-VCH GmbH

23667486, 0, Downloaded from https://onlinelibrary.wiley.com/doi/10.1002/adsu.202300366 by Koc University, Wiley Online Library on [23/03/2024]. See the Terms and Conditions (https://onlinelibrary.wiley.com/terms-and-conditions) on Wiley Online Library for rules of use; OA articles are governed by the applicable Creative Commons License

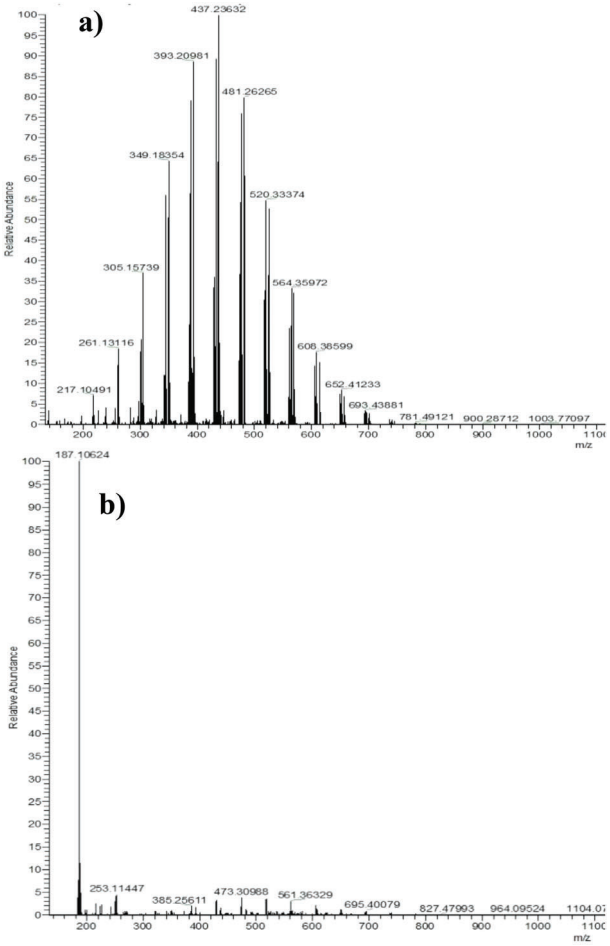


Figure 3. Comparison of LC-HRMS spectra of a) SL (the pristine lignin) and b) PSL (depolymerized lignin sample). The nature-inspired depolymerization of lignin by means of light-induced free radical-promoted cleavage reactions yields mainly guaiacyl alcohol; as evidenced by the value m/z = 187.10 corresponding to the lithium adduct of guaiacyl alcohol.

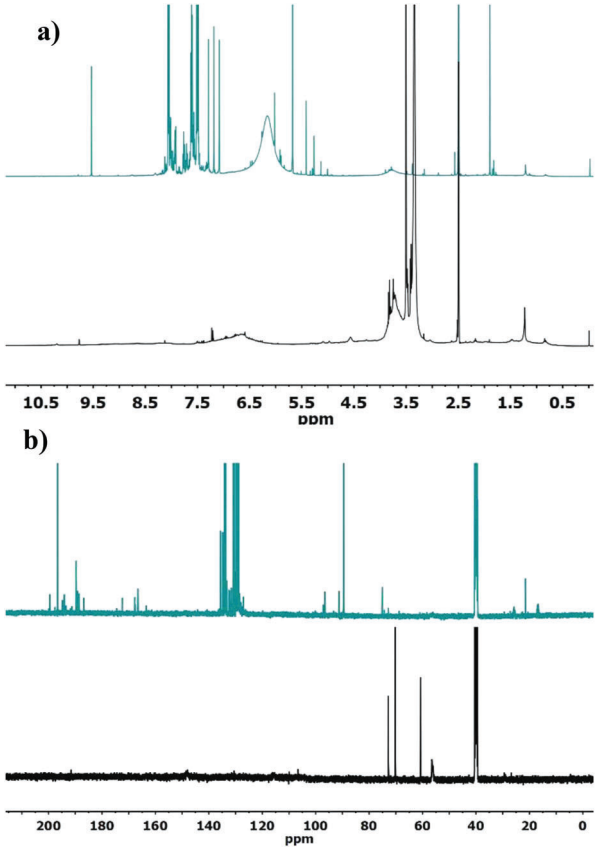


Figure 4. a) ^{1}H NMR spectra of (black) SL and (blue) PSL, b) ^{13}C NMR spectra of (black) SL and (blue) PSL (solvent: DMSO-d6).

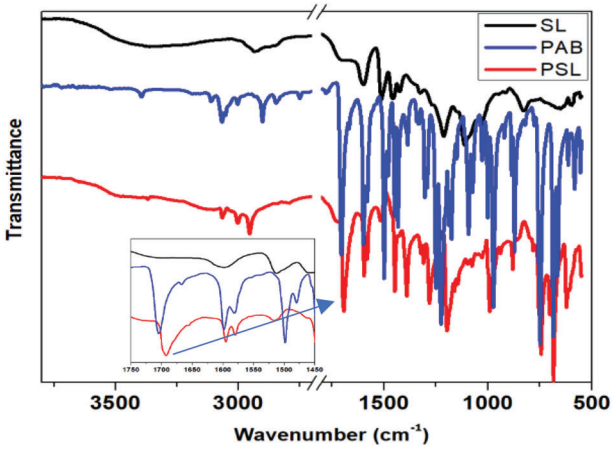


Figure 5. FT-IR spectra of (black) SL, (blue) PAB, and (red) PSL (inset image is focused on 1750–1400 cm^{-1}).

that aren't cleaved and which were also observable in GPC traces (Figure 2, inset photo).

Similarly, a comparison of ^{1}H and ^{13}C NMR spectra of SL and PSL (**Figure 4**a,b) revealed the formation of several aromatic aldehydes and carboxylic acids having proton peaks between 7.3–8.0 ppm and carbon peaks in 185–200 ppm region, respectively. The aromatic region in SL's spectrum is less apparent compared to the aromatic region in PSL's spectrum. This is due to the aggregation of phenolic units through $\pi-\pi$ stacking, resulting in poor solubility, as explained in the introduction part. Strong aromatic peaks in PSL's spectrum belong to the phenyl hydrogens of guaiacyl alcohol and other newly formed aromatic monomers and oligomers. The broad peak between 3.5-4 ppm can be associated with the methoxyl group (—OCH_3) of lignin units. The significant decrease in the area of methoxyl units from SL to PSL is attributed to the demethylation followed by phenolation reaction, as it was previously demonstrated that halogenic acids are effective in both increasing lignin hydroxyl group content and cleaving of β-O-4 bonds.[35] The chemical shifts in PSL spectrum between 4.0 – 6.0 ppm indicate the preservation of olefinic protons. Spectra observed at 7.7–7.3 ppm can be associated with guaiacyl unit. ^{1}H and ^{13}C NMR spectra of SL taken in CD_3CN can be found in Figure S10a,b (Supporting Information), respectively. A control experiment performed in the absence of PAB under identical conditions resulted in no change in the ^{1}H NMR spectrum (Figure S11, Supporting Information).

In the comparison of IR spectra of SL, PSL, and PAB (**Figure 5**), there is a significant change near 3000 cm^{-1} in the PSL spectrum

© 2023 The Authors. Advanced Sustainable Systems published by Wiley-VCH GmbH

23667486, 0, Downloaded from https://onlinelibrary.wiley.com/doi/10.1002/adsu.202300366 by Koc University, Wiley Online Library on [23/03/2024]. See the Terms and Conditions (https://onlinelibrary.wiley.com/terms-and-conditions) on Wiley Online Library for rules of use; OA articles are governed by the applicable Creative Commons License

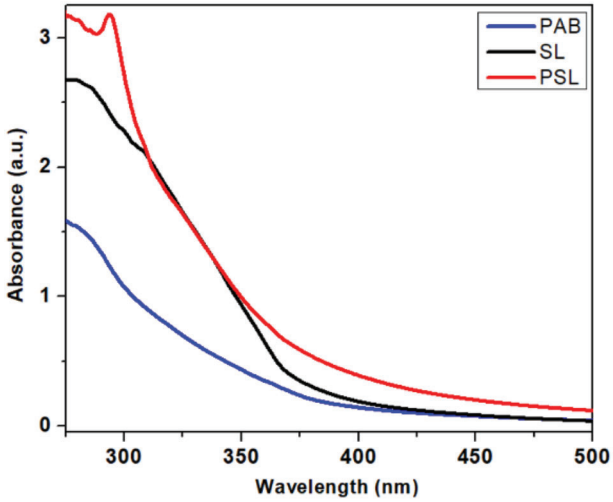


Figure 6. UV–vis spectra of (black) SL, (blue) PAB, and (red) PSL measured in DMSO solvent.

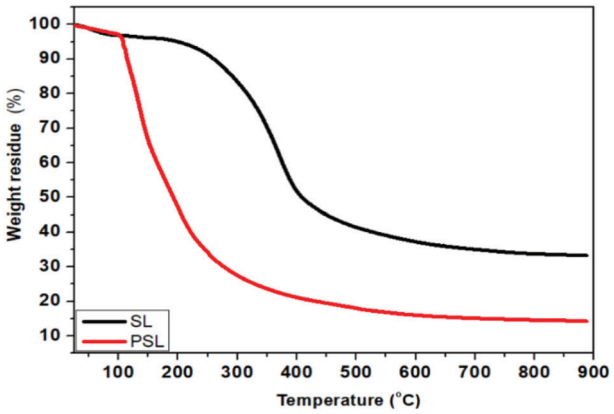


Figure 7. TGA thermograms of (black) SL and (red) PSL measured under a nitrogen atmosphere. Upon depolymerization, the sample (PSL) exhibits significantly less thermal stability than the sample that has not been depolymerized (SL).

corresponding to the aromatic C-H stretching peaks of newly formed aromatic species. In addition, the broad C═O stretching peak near 1700 cm^{-1} is due to different unconjugated carbonyl compounds (aldehydes and quinones) and indicates the formation of new aromatic aldehyde and carboxylic acid species as this was also evidenced in the ^{13}C NMR spectrum of PSL (Figure 4b). The relative values of the peaks at 1458 cm^{-1} in SL, corresponding to C—O deformation of methoxyl group decreased significantly in PSL due to demethylation/phenolation by HBr.

A comparison of UV–vis spectra of SL and PSL revealed the significantly higher UV absorption of PSL compared to that of SL (**Figure 6**). The absorption peak around 290 nm corresponds to the characteristics of phenolic groups. Higher absorption of PSL in 300 nm and visible region is due to the formation of new products with lower molecular weights, that are rich in carbonyl and phenolic groups such as o-quinones.

The crystallinity of SL and PSL were investigated using powder X-ray diffractometry (PXRD) (Figure S11, Supporting Information). While SL exhibited a totally amorphous structure with no assignable peaks, PSL revealed sharp peaks corresponding to crystalline monomeric species and a broad peak ≈26°. This broad peak is due to the breaking of the cross-linked bonds of SL forming monomeric and oligomeric molecules which stack through weak $\pi-\pi$ interactions.[36]

Thermal stabilities of SL and PSL were probed by employing TGA (thermal gravimetric analysis) (**Figure 7**) and DSC (differential scanning calorimetry) measurements (Figure S12, Supporting Information). Examination of TGA thermograms disclosed the occurrence of first weight loss (≈4%) in both compounds between 50–100 °C due to the evaporation of absorbed water. Remarkable amount of absorbed water in both SL and PSL can be related to the hygroscopic functional groups such as phenolics, forming hydrogen bonds with ambient water molecules.[37] A significant change can be observed starting from 100 °C when thermograms of SL and PSL are compared. While SL possessing a cross-linked structure showed thermal stability up to 300 °C (only ≈%10 weight loss), PSL lost most of its weight (≈73%) at that temperature. This huge weight loss is a consequence of the boiling of different monomeric species produced by the successive photo-depolymerization of SL. After 300 °C, while SL underwent a rapid pyrolytic degradation, PSL's weight loss was much smaller. The efficient depolymerization process of SL was also supported by DSC results (Figure S13, Supporting Information). Endothermic peaks in both compounds, starting from 75 °C stand for the gradual evaporation of the ambient water absorbed by phenolic monomers. However, after 100 °C, there is a notable change between the DSC curves of SL and PSL. While PSL exhibited a broad exothermic peak between 75–150 °C corresponding to the melting points of monomeric species, SL exhibited no obvious exothermic peak after 100 °C due to its cross-linked nature.

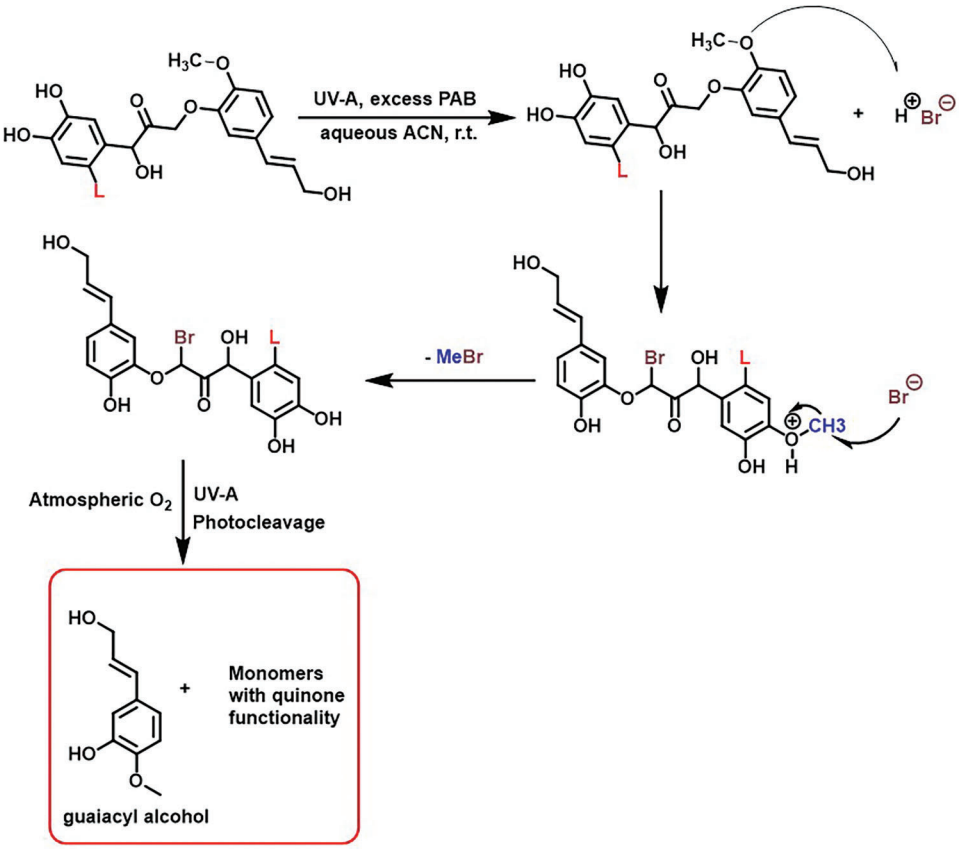
Based on all the spectral, chromatographic, and thermal investigations, we propose the following reaction mechanisms which are depicted in **Scheme 3**.

3. Conclusion

In conclusion, we have originated a sustainable valorization strategy for the transformation of soda lignin to guaiacyl alcohol. Photoreaction between model compound (2-PAP) and PAB was investigated using real-time NMR, LC-HRMS, and GPC in order to understand the reaction mechanisms. Besides guaiacyl alcohol, photoconversion of soda lignin to a trace amount of monomers/oligomers that are rich in carbonyl functionalities supported our proposed mechanism of the model compound reaction in which the consumption of β-O-4 motifs, in the presence of molecular oxygen, led to the formation of carbonyl-containing species. The unprecedented performance of PAB-inducing β-O-4 scission can be qualitatively rationalized by the formation of photolabile brominated compounds. Initially formed brominated lignin moieties result in the inhibition of aggregation, leading to a significant increase in solubility. Furthermore, the generation of HBr through the hydrogen abstraction of photolytically generated bromine radicals should have a synergistic influence on the depolymerization process through demethylation/phenolation. In short, the critical advancement of this work is the demonstration of a sustainable approach for technical lignin valorization under mild conditions.

© 2023 The Authors. Advanced Sustainable Systems published by Wiley-VCH GmbH

23667486, 0, Downloaded from https://onlinelibrary.wiley.com/doi/10.1002/adsu.202300366 by Koc University, Wiley Online Library on [23/03/2024]. See the Terms and Conditions (https://onlinelibrary.wiley.com/terms-and-conditions) on Wiley Online Library for rules of use; OA articles are governed by the applicable Creative Commons License



Scheme 3. Plausible mechanism for the light-induced depolymerization of soda lignin, yielding guaiacyl alcohol as the main product.

4. Experimental Section

Materials: 2-bromoacetophenone (98%, phenacyl bromide or PAB) was purchased from Sigma and was recrystallized from hot absolute ethanol solution prior to use. 2-phenoxyacetophenone (100%) was purchased from Sigma-Aldrich and used without any purification. Soda lignin was obtained from industrial pulping spent liquor. Technical grade acetonitrile (97%) was used as received. Deuterated acetonitrile (CD_3CN, 99%), chloroform ($CDCl_3$, 99.8%), and dimethyl sulfoxide (DMSO-d6, 99.8%) were purchased from Merck and used as received.

Instrumentation: A photoreactor equipped with a magnetic stirrer, cooling fan, and 18 fluorescent lamps (Philips TL 18 W BLB) emitting light nominally at 355 nm with a light intensity of 100 mW cm^{-2} at reaction flask, was used for all the reactions. Gel-permeation chromatography (GPC) measurements were performed using a TOSOH EcoSEC GPC system equipped with an auto-sampler system, a temperature-controlled pump, a column oven, refractive index(RI) and light-scattering (LS) detectors, a purge and degasser unit, and a TSKgel superhZ2000 4.6 mm ID × 15 cm × 2 cm column. Tetrahydrofuran (THF) was used as an eluent at a flow rate of 1.0 mL· min^{-1} at 40 °C. The refractive index detector was calibrated with polystyrene standards having narrow molecular-weight distributions. GPC data were analyzed by using Eco-SEC Analysis software. UV–Vis spectra were recorded using an Agilent Carry UV–Vis–NIR double-beam spectrometer equipped with a 50 W halogen lamp and a deuterium lamp which could operate between 200 and 1100 nm. ^1H NMR spectra were recorded in deuterated acetonitrile and chloroform (CD_3CN and $CDCl_3$ with tetramethylsilane as an internal standard) at 500 MHz on an Agilent VNMRS 500 spectrometer at 25 °C. Fourier-transform infrared (IR) spectra were recorded on a PerkinElmer Spectrum One spectrometer equipped with an ATR accessory (ZnSe, PikeMiracle) and a mercury cadmium telluride (MCT) detector. A total of 32 scans were averaged. The liquid-chromatography analyses were performed with reversed-phase liquid chromatography coupled to high-resolution mass spectrometry (LC-HRMS Thermo Q Exactive, Thermo Fisher Scientific Inc, Waltham, USA). Acquisition of raw LC-HRMS data was performed in full scan mode at a resolution of 35 000 with polarity switching. Direct injection LC-HRMS data were recorded on Thermo LCQ-Deca ion trap mass instrument. Crystallographic investigation was accomplished by powder X-ray diffraction (PXRD) method on a Bruker D2 Advanced X-ray diffractometer with a Cu-Kα radiation source operated at 30 kV and 10 mA. The acquisition angle ranged from 10° to 90°, where each step was processed with a 0.05° increment. Thermogravimetric analysis (TGA) was performed on a Perkin-Elmer Diamond TA/TGA with a heating rate of 10 K·min^{-1} under a nitrogen flow of 200 mL·min^{-1}. Differential scanning calorimetry (DSC) measurements were performed on a Perkin Elmer Diamond DSC 4000 with a heating rate of 10 K·min^{-1} under a nitrogen flow of 20 mL·min^{-1}. pH measurements were done using a Hanna HI 2211 device calibrated with pH = 4,7,10 buffer solutions.

Supporting Information

Supporting Information is available from the Wiley Online Library or from the author.

Acknowledgements

The authors thank Binnur Aydogan Temel and Tugser Yilmaz, Umut Aydemir for their help in LC-HRMS and PXRD measurements, respectively. This work was supported by the Istanbul Technical University Research Fund and the Turkish Council of Higher Education (YÖK) Project No: YAP-44004.

© 2023 The Authors. Advanced Sustainable Systems published by Wiley-VCH GmbH

23667486, 0, Downloaded from https://onlinelibrary.wiley.com/doi/10.1002/adsu.202300366 by Koc University, Wiley Online Library on [23/03/2024]. See the Terms and Conditions (https://onlinelibrary.wiley.com/terms-and-conditions) on Wiley Online Library for rules of use; OA articles are governed by the applicable Creative Commons License

Conflict of Interest

The author declares no conflicts of interest.

Data Availability Statement

The data that support the findings of this study are available from the corresponding author upon reasonable request.

Keywords

biomasses, guaiacyl alcohols, light-induced free-radical promoted cleavages, soda lignins, valorization

Received: August 12, 2023
Revised: September 5, 2023
Published online:

[1] J. Hansen, P. Kharecha, M. Sato, V. Masson-Delmotte, F. Ackerman, D. J. Beerling, P. J. Hearty, O. Hoegh-Guldberg, S.-L. Hsu, C. Parmesan, J. Rockstrom, E. J. Rohling, J. Sachs, P. Smith, K. Steffen, L. Van Susteren, K. Von Schuckmann, J. C. Zachos, *PLoS One* **2013**, *8*, 81648.

[2] C. Román-Palacios, J. J. Wiens, *Proc. Natl. Acad. Sci. USA* **2020**, *117*, 4211.

[3] a) D. Haldar, M. K. Purkait, *Chemosphere* **2021**, *264*, 128523; b) T. M. Budnyak, A. Slabon, M. H. Sipponen, *ChemSusChem* **2020**, *13*, 4344; c) A. Moreno, J. Liu, R. Gueret, S. E. Hadi, L. Bergström, A. Slabon, M. H. Sipponen, *Angew.Chem.Int. Ed* **2021**, *60*, 20897; d) L. Lindenbeck, B. B. Beele, M. Morsali, S. Budnyk, M. Frauscher, J. Chen, M. H. Sipponen, A. Slabon, B. V. M. Rodrigues, *Nanoscale* **2023**, *15*, 9014.

[4] C. G. Yoo, X. Meng, Y. Pu, A. J. Ragauskas, *Bioresour.Technol* **2020**, *301*, 122784.

[5] a) A. De Santi, S. Monti, G. Barcaro, Z. Zhang, K. Barta, P. J. Deuss, *ACS Sustainable Chem. Eng.* **2021**, *9*, 2388; b) G. T. Beckham, C. W. Johnson, E. M. Karp, D. Salvachúa, D. R. Vardon, *Curr. Opin. Biotechnol.* **2016**, *42*, 40; c) C. Weng, X. Peng, Y. Han, *Biotechnol. for Biofuels* **2021**, *14*, 84.

[6] a) Y. Lu, Y.-C. Lu, H.-Q. Hu, F.-J. Xie, X.-Y. Wei, X. Fan, *J. Spectroscopy* **2017**, *2017*, 8951658; b) S. H. Ghaffar, M. Fan, *Biomass Bioenergy* **2013**, *57*, 264.

[7] a) A. Eraghi Kazzaz, P. Fatehi, *Ind. Crops. Prod.* **2020**, *154*, 112732; b) T. Li, S. Takkellapati, *Biofuel Bioprod Biorefin* **2018**, *12*, 756.

[8] a) P. Prinsen, J. Rencoret, A. Gutiérrez, T. Liitiä, T. Tamminen, J. L. Colodette, M. Á. Berbis, J. Jiménez-Barbero, Á. T. Martínez, J. C. Del Río, *Ind. Eng. Chem. Res.* **2013**, *52*, 15702; b) N. Kumar, S. Vijayshankar, P. Pasupathi, S. Nirmal Kumar, P. Elangovan, M. Rajesh, K. Tamilarasan, *Res. Chem. Intermed.* **2018**, *44*, 5403.

[9] J. Lu, M. Wang, X. Zhang, A. Heyden, F. Wang, *ACS Catal.* **2016**, *6*, 5589.

[10] a) X. Liu, F. P. Bouxin, J. Fan, V. L. Budarin, C. Hu, J. H. Clark, *ChemSusChem* **2020**, *13*, 4296; b) T. Rinesch, C. Bolm, *ACS Omega* **2018**, *3*, 8386; c) I. Romanenko, F. Kurz, R. Baumgarten, I. Jevtovikj, J.-P. Lindner, A. Kundu, A. Kindler, S. A. Schunk, *Catalysts* **2022**, *12*, 158; d) D. Bourbiaux, J. Pu, F. Rataboul, L. Djakovitch, C. Geantet, D. Laurenti, *Catal. Today* **2021**, *373*, 24; e) E. Subbotina, T. Rukkijakan, M. D. Marquez-Medina, X. Yu, M. Johnsson, J. S. M. Samec, *Nat. Chem.* **2021**, *13*, 1118.

[11] a) F. Lin, H.-Y. Tse, H. C. Erythropel, P. V. Petrović, M. Garedew, J. Chen, J. C.-H. Lam, P. T. Anastas, *Green Chem.* **2022**, *24*, 6295; b) C. Yang, M. D. Kärkäs, G. Magallanes, K. Chan, C. R. J. Stephenson, *Org. Lett.* **2020**, *22*, 8082.

[12] X. Liu, L. Wang, L. Zhai, C. Wu, H. Xu, *Green Chem.* **2022**, *24*, 4395.

[13] a) C. Liu, S. Wu, H. Zhang, R. Xiao, *Fuel Process. Technol.* **2019**, *191*, 181; b) R. Ma, M. Guo, X. Zhang, *Catal. Today* **2018**, *302*, 50.

[14] a) M. G. A. Da Cruz, R. Gueret, J. Chen, J. Piatek, B. Beele, M. H. Sipponen, M. Frauscher, S. Budnyk, B. V. M. Rodrigues, A. Slabon, *ChemSusChem* **2022**, *15*, 202200718; b) M. G. A. da Cruz, B. V. M. Rodrigues, A. Ristic, S. Budnyk, S. Das, A. Slabon, *GCLR* **2022**, *15*, 153.

[15] I. T. Horváth, *Chem. Rev.* **2018**, *118*, 369.

[16] a) T. Chen, H. Wang, Y. Chu, C. Boyer, J. Liu, J. Xu, *ChemPhotoChem* **2019**, *3*, 1059; b) H. Wang, G. J. Giardino, R. Chen, C. Yang, J. Niu, D. Wang, *ACS Cent. Sci.* **2023**, *9*, 48; c) J. Xu, M. Li, J. Qiu, X.-F. Zhang, J. Yao, *Int. J. Biol. Macromol.* **2021**, *180*, 403; d) C. A. Boyer, G. M. Miyake, *Macromol. Rapid Commun.* **2017**, *38*, 1700327.

[17] a) S. Li, Z. Hao, K. Wang, M. Tong, Y. Yang, H. Jiang, Y. Xiao, F. Zhang, *ChemComm* **2020**, *56*, 11243; b) J. Luo, X. Zhang, J. Lu, J. Zhang, *ACS Catal.* **2017**, *7*, 5062; c) Y. Kang, X. Lu, G. Zhang, X. Yao, J. Xin, S. Yang, Y. Yang, J. Xu, M.i Feng, S. Zhang, *ChemSusChem* **2019**, *12*, 4005.

[18] a) O. Lanzalunga, M. Bietti, *J. Photochem. Photobiol. B, Biol.* **2000**, *56*, 85; b) Y. pu, L. Anderson, L. Lucia, A. Ragauskas, *J. Pulp Paper Sci.* **2003**, *29*, 401; c) J. H. Zhu, D. G. Gray, *J. Photochem. Photobiol. A: Chem.* **1995**, *87*, 267.

[19] a) A. Cogulet, P. Blanchet, V. Landry, *J. Photochem. Photobiol. B, Biol.* **2016**, *158*, 184; b) M. Paulsson, J. Parkås, *BioResources* **2012**, *7*, 5995.

[20] H. Sadeghifar, A. Ragauskas, *Polymers (Basel)* **2020**, *12*, 1134.

[21] a) Y. Qian, X. Qiu, S. Zhu, *Green Chem.* **2015**, *17*, 320; b) P. Widsten, *Cosmetics* **2020**, *7*, 85.

[22] a) H.-I. Joschek, S. I. Miller, *JACS* **1966**, *88*, 3269; b) A. Saeed, M. Altarawneh, K. Siddique, J. A. Conesa, N. Ortuño, B. Z. Dlugogorski, *Ecotoxicol. Environ. Saf.* **2020**, *192*, 110272.

[23] A. Khaled, A. Rivaton, C. Richard, F. Jaber, M. Sleiman, *Environ. Sci. Technol.* **2018**, *52*, 11123.

[24] A. Segura-Quezada, Y. Satkar, D. Patil, N. Mali, K. Wrobel, G. González, R. Zárraga, R. Ortiz-Alvarado, C. R. Solorio-Alvarado, *Tetrahedron Lett.* **2019**, *60*, 1551.

[25] a) W. Zhao, L.-P. Xiao, G. Song, R.-C. Sun, L. He, S. Singh, B. A. Simmons, G. Cheng, *Green Chem.* **2017**, *19*, 3272; b) J. Domínguez-Robles, T. Tamminen, T. Liitiä, M. S. Peresin, A. Rodríguez, A.-S. JääSkeläinen, *Int. J. Biol. Macromol.* **2018**, *106*, 979.

[26] J. Wang?, Y. Hou, W. Lei, Q. Zhou, C. Li, B. Zhang, X. Wang, *ChemPhysChem* **2012**, *13*, 2739.

[27] a) K. Kaya, J. Kreutzer, Y. Yagci, *ChemPhotoChem* **2019**, *3*, 1187; b) K. Kaya, S. Koyuncu, Y. Yagci, *ChemComm* **2019**, *55*, 11531.

[28] a) A. Kocaarslan, K. Kaya, S. Jockusch, Y. Yagci, *Angew. Chem., Int. Ed.* **2022**, *61*, e202208845; b) K. Kaya, *React. Funct. Polym.* **2023**, *182*, 105464.

[29] W. G. Mcgimpsey, J. C. Scaiano, *Can. J. Chem.* **1988**, *66*, 1474.

[30] W.-Y. Song, H. Park, T.-Y. Kim, *J. Chromatogr. A* **2022**, *1685*, 463598.

[31] M. D'auria, L. Emanuele, R. Racioppi, *Nat. Prod. Res.* **2012**, *26*, 1368.

[32] K. R. Dean, B. C. Lynn, *Int. J. Mass. Spectrom.* **2019**, *442*, 109.

[33] D. R. Letourneau, D. A. Volmer, *Mass Spectrom. Rev.* **2023**, *42*, 144.

[34] A. Kruve, K. Kaupmees, *J. Am. Soc. Mass Spectrom.* **2017**, *28*, 887.

[35] a) H. Wang, T. L. Eberhardt, C. Wang, S. Gao, H. Pan, *Polymers* **2019**, *11*, 1771; b) Y. Wang, M. Chen, Y. Yang, J. Ralph, X. Pan, *RSC Adv.* **2023**, *13*, 5925; c) Z. Li, E. Sutandar, T. Goihl, X. Zhang, X. Pan, *Green Chem.* **2020**, *22*, 7989.

[36] A. K. Singh, S. K. Katari, A. Umamaheswari, A. Raj, *RSC Adv.* **2021**, *11*, 14632.

[37] B. Jadhav, R. Roy, M. S. Rahman, D. E. Raynie, *Biomass* **2022**, *2*, 348.

© 2023 The Authors. Advanced Sustainable Systems published by Wiley-VCH GmbH

23667486, 0, Downloaded from https://onlinelibrary.wiley.com/doi/10.1002/adsu.202300366 by Koc University, Wiley Online Library on [23/03/2024]. See the Terms and Conditions (https://onlinelibrary.wiley.com/terms-and-conditions) on Wiley Online Library for rules of use; OA articles are governed by the applicable Creative Commons License